Endocytosis in Filter-grown Madin–Darby Canine Kidney Cells

Morgane Bomsel,* Kristian Prydz, Robert G. Parton, Jean Gruenberg, and Kai Simons

European Molecular Biology Laboratory, Federal Republic of Germany; Postfach 10.2209, D-6900 Heidelberg, Federal Republic of Germany; and *ER64-Centre Nationale la Recherche Scientifique, Etats Liés Moleculaires, F-75006 Paris, France

Abstract. In this paper, we have characterized the apical and basolateral endocytic pathways of epithelial MDCK cells grown on filters. The three-dimensional organization of the endocytic compartments was analyzed by confocal microscopy after internalization of a fluorescent fluid-phase marker from either side of the cell layer. After 5 min of internalization, distinct sets of apical and basolateral early endosomes were observed lining the plasma membrane domain from which internalization had occurred. At later time points, the apical and the basolateral endocytic pathways were shown to converge in the perinuclear region. Mixing of two different fluorescent markers could be detected after their simultaneous internalization from opposite sides of the cell layer. The extent of the meeting was quantitated by measuring the amount of complex formed intracellularly between avidin internalized from the apical side and biotinylated horseradish peroxidase (HRP) from the basolateral side. After 15 min, 14% of the avidin marker was complexed with the biotinylated HRP and this value increased to 50% during a subsequent chase of 60 min in avidin-free medium. We also determined the kinetics of fluid internalization, recycling, transcytosis, and intracellular retention using HRP as a marker. Fluid was internalized with the same rates from either surface domain (1.2×10^{-4} μm^3/min per μm^2 of surface area). However, significant differences were observed for each pathway in the amounts and kinetics of marker recycled and transcytosed. The content of apical early endosomes was primarily recycled and transcytosed (45% along each route after 1 h internalization), whereas delivery to late endocytic compartments was favored from the basolateral early endosome (77% after 1 h). Our results demonstrate that early apical and basolateral endosomes are functionally and topologically distinct, but that the endocytic pathways converge at later stages in the perinuclear region of the cell.

THE analysis of the endocytic pathway in simple epithelia is complicated by the polar organization of the cell layer. Epithelial cells, lining the body cavities, form sheets between the external and internal environments. As a result of these boundary functions, epithelial cells have evolved two specialized plasma membrane domains with distinct protein and lipid compositions (Simons and Fuller, 1985). The apical membrane confronts the outside world, whereas the basolateral domain faces the basement membrane and the blood supply. The specificity of these two domains is maintained by tight junctions, which form a fence to prevent mixing of apical and basolateral membrane components as well as an occluding barrier between neighboring cells (Gumbiner, 1987).

Endocytosis is known to occur from both the apical and the basolateral surfaces (Simons and Fuller, 1985). There is another major difference from nonpolarized cells (Courtoy, 1989; Gruenberg and Howell, 1989). Molecules endocytosed by epithelial cells are not only recycled or transported to lysosomes for degradation but can also be transcytosed to the opposite cell surface via a transcellular vesicular route (Mostov and Simister, 1985). Nevertheless, despite continuous endocytosis and transcytosis, epithelial surface polarity is maintained. How this is achieved is not known, nor is the overall organization of the endocytic pathways in simple epithelia well characterized. Most of the studies on endocytosis in simple epithelial cells (Abrahamson and Rodewald, 1981; Christensen, 1982; Herzog, 1984; Gonnella and Neutra, 1984; van Deurs and Christensen, 1984) have been performed on whole tissues where access to both sides of the epithelium is difficult to control. In both isolated rabbit proximal tubules (Nielsen et al., 1985) and in the rat parotid acinar gland (Oliver, 1982), ferritin internalized from the apical membrane domain and horseradish peroxidase (HRP)[1] endocytosed from the basolateral membrane were routed to the same lysosomes. However, the extent of meeting was not quantitated nor was the site of convergence identified.

We have grown MDCK strain I cells on permeable polycarbonate supports to gain experimental access to both apical and basolateral plasma membrane domains independently.

1. *Abbreviations used in this paper*: bBSA, biotinylated BSA; bHRP, biotinylated horseradish peroxidase; HRP, horseradish peroxidase; IM, internalization medium; LY, Lucifer yellow; PBS^+, PBS with 1 mM Ca^{2+} and 0.5 mM Mg^{2+}.

Under these conditions, the cells form a monolayer with very high transepithelial resistance that closely mimics the epithelial organization observed in vivo (Richardson et al., 1981; Fuller et al., 1984). In this study, we have extended our previous work on endocytosis in filter-grown MDCK cells (von Bonsdorff et al., 1985). The topology of the apical and basolateral endocytic compartments was analyzed after internalization of fluorescent fluid phase markers from either surface domain. The spatial distribution of the markers within the cell was visualized by confocal fluorescence microscopy, coupled to three-dimensional image reconstruction. The different routes accessible to the internalized fluid phase markers were assessed using two biochemical approaches. Internalization from either cell surface domain and subsequent recycling, transcytosis, and transport to later endocytic compartments were quantitated with HRP. The extent of the meeting of the apical and basolateral pathways was measured using avidin and biotinylated HRP internalized from opposite sides of the cell layer. In a companion paper, the organization and the meeting of the endocytic pathways were further studied by EM.

Materials and Methods

Materials

Dextran-Texas Red (molecular weight 10,000) was purchased from Molecular Probes, Inc. (Eugene, OR) and was purified on a Sephadex G-50 (Pharmacia Fine Chemicals, Uppsala, Sweden) column, dried from acetone, and stored at −20°C. Lucifer yellow (LY), wheat germ agglutinin (WGA)-Texas Red, ribonuclease A (RNase), avidin (egg white), HRP (type II), 1,4-diazabicyclo(2.2.2)octane (DABCO), and BSA (essentially fatty acid free, fraction V) were obtained from Sigma Chemical Co. (St. Louis, MO). LY was inactivated in methanol/acetone (2:1), dried under N_2, and stored at −20°C. Glycerol (87%) was obtained from E. Merck (Darmstadt, FRG). Biotin-ε-aminocaproic acid-*N*-hydroxysuccinimide ester (biotin-X-NHS) was from Calbiochem-Behring Corp., (Frankfurt, FRG). Proteins were biotinylated as described (Gruenberg et al., 1989). A polyclonal antibody against avidin was raised in rabbits and affinity purified.

Cells

MDCK strain I cells (Richardson et al., 1981), subcloned by Fuller et al. (1984) were maintained in 75-cm^2 flasks in a 5% CO_2 atmosphere at 37°C and the medium was Earle's MEM, containing 10% FCS, 2 mM glutamine, 100 U/ml penicillin, and 100 U/ml streptomycin. At confluency (1.5×10^7 cells per flask), the cells were trypsinized and resuspended in 10 ml medium 1.6 ml of which was added to the apical side of a polycarbonate filter (4.7 cm^2, Transwell, 0.4 μm pore size; Costar Corp., Cambridge, MA). The filters were then mounted on polypropylene holders, and placed in a set of six in a 150-mm Petri dish with 90 ml medium. Transepithelial resistance across the cell monolayer was measured before each experiment (Fuller et al., 1984) and filters with values >2,000 Ω × cm^2 were used (3–4 d after seeding). Essentially no fluid leaked between the cells in a filter-grown monolayer of the tight MDCK I cells (von Bonsdorff et al., 1985).

Uptake of Fluorescent Fluid Phase Markers

For apical uptake, the cells on filters were briefly rinsed in incubation medium (IM-F; MEM, 0.05% BSA, buffered with 10 mM Hepes to pH 7.4) at 37°C. The filters were then placed in six-well plates (Costar Corp.) containing 2 ml IM-F in each well and prewarmed in a 37°C water bath. After two brief washes with prewarmed IM-F, 10 mg/ml LY in 500 μl IM-F was added to the apical side. For basolateral uptake, the edge of the filters on the side opposite to the cells was carefully blotted with a filter paper to remove excess basolateral medium. The filter was placed onto a 100-μl drop of 10 mg/ml LY in IM-F prewarmed at 37°C on a piece of parafilm in a humid chamber. Then 800 μl of prewarmed IM-F was added to the apical side and incubation was carried out for the desired time. For simultaneous internalization from the apical and the basolateral side, 10 mg/ml dextran-Texas Red and 10 mg/ml LY were added to the apical and the basolateral medium, respectively. For the labeling of late endocytic compartments, the marker was first internalized for 30 min, then the cells were washed briefly and further incubated in marker-free IM-F for an additional hour. All incubations were terminated by four 10-min washes in ice-cold PBS^+ (PBS with 1 mM Ca^{2+}, 0.5 mM Mg^{2+}) containing 0.5% BSA (PBS^+-BSA) before fixation.

Fixation of Cells for Confocal Microscopy

The polycarbonate filters were briefly rinsed in PBS^+ at 4°C. All subsequent steps were at room temperature. The fixation was performed in a two-step procedure, adapted from Berod et al. (1981). First, the cells were immersed in 3.7% paraformaldehyde in 80 mM Pipes, pH 6.5 (5 mM EGTA, 2 mM $MgCl_2$) for 4 min to allow the paraformaldehyde to penetrate the cells. The filters were then transferred to 3.7% paraformaldehyde in 100 mM sodium borate (pH 11) to promote polymerization of the paraformaldehyde. After 8 min, the cells were rapidly washed three times in PBS^+ and the free aldehydes were quenched with 75 mM NH_4Cl and 20 mM glycine in PBS^+ for 10 min. The fixation procedure ended by three 10-min washes in PBS^+. Then the filters were mounted on coverslips in PBS^+ containing 50% glycerol as well as 100 mg/ml DABCO to reduce photobleaching (Langanger et al., 1983). The height of the cells after fixation and mounting was similar, within 5%, to that of unfixed cells, a good indication that the three-dimensional cellular organization had been preserved. In addition, electron microscopic examination of the cells after fixation showed no major alterations of the cellular organization when compared with control cells fixed in glutaraldehyde, as in Parton et al. (1989).

Fluorescent Labeling of Other Organelles

mAbs have been used to visualize the distribution of the 114-kD protein (Balcarova-Ständer et al., 1984), uvomorulin (Gumbiner and Simons, 1986), or nuclear lamin B (Lehner et al., 1986) by indirect immunofluorescence. The detecting antibody was an anti-mouse IgG coupled to either rhodamin or Texas Red (Dianova, Hamburg, FRG). To stain the basolateral plasma membrane after uptake of the fluorescent fluid phase marker, the cells were washed in PBS^+-BSA at 4°C and the basolateral medium was replaced by PBS^+-BSA containing 50 μg/ml WGA-Texas Red. The cells were further incubated for 1 h at 4°C, washed three times in PBS^+-BSA, and fixed as above. To stain the nuclei, the cells were first fixed as above, then treated with 1 mg/ml RNase in PBS for 20 min at room temperature. After three brief washes in PBS^+, the cells were treated with 2 μg/ml propidium iodide in PBS^+ for 15 min at room temperature.

Confocal Scanning Beam Laser Microscopy

A description of design and operating principles of the confocal microscope developed at the European Molecular Biology Laboratory has been published previously (Stelzer et al., 1989). Two wavelengths (476 and 514.5 nm) out of several lines produced by an argon laser (model 2020-05; Spectra Physics) were used to excite LY and Dextran-Texas Red, respectively. Emitted or reflected light was detected with a photomultiplier (model R1463-01; Hamamatsu, Hamamatsu City, Japan) located behind a fixed size pinhole. Images of several optical sections (0.4 μm resolution on the vertical axis) were stored in a microcomputer (model VME 6800; Eltec, Mainz, FRG). One image was composed of 512 × 512 pixels. The images were photographed using a black and white monitor (Knott elektronik, Ismaningen, FRG) and a prefocused Minolta X-300 camera. Kodak T-Max 100 film (Eastman Kodak Co., Rochester, NY) was used for single-labeled images. The image analysis was performed with programs established by C. Storz and E. Stelzer (European Molecular Biology Laboratory, Heidelberg, FRG). The resulting images were photographed using Fujichrome DX 400 film. The stereo images presented in this paper are preferably viewed with stereoscopes (Hubbard Scientific Co., Northbrook, IL).

Continuous Uptake Measurement with HRP

The same experimental protocol was used as for the uptake of fluorescent markers from both sides of the cell layer, except that phenol red was omitted from the internalization medium (IM-H). For internalization experiments, the filters were incubated in IM-H containing 2–10 mg/ml HRP. Typically, the volumes were 400 and 200 μl for the apical and the basolateral medium, respectively, and HRP was present at either side as indicated. After internalization, the apical and basolateral media were collected and centrifuged at 3,000 *g* for 5 min to remove any debris. Cells were cooled to 4°C in

PBS^+-BSA and washed in the same medium four times for 10 min each. The total amount of HRP present in the cells was obtained after extraction for 45 min at 4°C with 500 μl lysis buffer (1% wt/vol Triton X-100, 0.5% wt/vol SDS) as described by von Bonsdorff et al. (1985). The enzymatic activity of HRP was then determined in the three fractions (apical and basolateral media, cell extract) according to Steinman et al. (1976).

Recycling and Transcytosis of HRP after Internalization

Cells were loaded for the desired time with HRP as described above. After extensive washing (four times for 10 min each) with PBS^+-BSA at 4°C, the cell monolayers were returned to 37°C in a humid chamber and further incubated for various times in IM-H. The apical and basolateral volumes were 300 and 200 μl, respectively. The apical and basolateral media were collected, the cells were extracted, and HRP enzymatic activity was determined as above.

The following controls were performed. First, in parallel experiments, the transepithelial resistance of the cells was checked after each experimental step, uptake at 37°C, washing at 4°C, and reincubation in marker-free medium; in all cases, the transepithelial resistance was >1,000 $\Omega \cdot cm^2$. Second, the HRP enzymatic activity determined in the media and in the cells increased linearly, when the HRP concentration in the uptake medium was increased from 2 to 10 mg/ml (data not shown). Third, both loading of the cells with HRP and re-incubation in marker-free medium were carried out at 4°C to estimate the amount of HRP nonspecifically adsorbed to cells or to the filters. With these conditions, no significant HRP activity was detected in the cell extract (<3% of the value at 37°C for each time point considered, respectively) or the media (<0.5% of the value at 37°C for each time point considered, respectively). Thus, the polycarbonate filters could be very efficiently washed, in agreement with the findings of Sargiacomo et al. (1989). Finally, two further controls was carried out to guarantee that HRP detected in the medium in the preloading-chase experiments was not due to the release of HRP adsorbed onto the cell surface. (*a*) The cells were preloaded for each time period with HRP at 37°C and after washing at 4°C and reincubated for 5–10 s at 37°C in marker-free medium. After this short chase period, no HRP activity was detected in the apical or the basolateral medium and the HRP activity associated with the cell monolayer extract was within 3% of the value obtained without this short treatment. (*b*) When reincubation in marker-free medium was performed at 4°C, the HRP activity detected was within 3% of that detected directly after loading at 37°C.

Biochemical Detection of the Meeting of the Two Endocytic Pathways

The experimental protocol was the same as described for the uptake of fluorescent markers from both sides of the cell layer, except that IM-F was replaced by IM-M (MEM containing 0.35 g HCO_3^-/liter and supplemented with 0.2% BSA and 10 mM Hepes). Typically, 400 μl of IM-M containing 2 mg/ml avidin was added apically, and the filter was placed on a drop (150 μl) of medium containing 2 mg/ml of the basolateral marker, biotinylated HRP (bHRP). The incubation was stopped by transferring the filters to a cold plate at 4°C. The apical medium containing avidin was replaced by the same volume of biotinylated BSA (bBSA) in PBS^+ (0.5 mg/ml) for 30 min at 0–4°C, to quench avidin possibly adsorbed to the cell surface. The filters were washed twice with ice-cold 0.2% BSA in PBS^+, cut out of their holders, and washed six times for 30 min each in 5 ml 0.2% BSA in PBS^+ with shaking. The filters were blotted to remove excess solution and extracted with 200 μl lysis buffer for 30 min at 4°C. Solubilization was carried out in the presence of bBSA (0.5 mg/ml) so that the formation of the avidin-bHRP complex could only result from meeting in vivo during endocytosis, before detergent solubilization. To determine the total amount of avidin present in the cells, bBSA was omitted, allowing binding of avidin to internalized bHRP present in the lysate. Exogeneous bHRP added to the lysate did not bind avidin (data not shown), suggesting that the amount of bHRP present in the lysate was sufficient to saturate avidin. Lysosomal degradation was not likely to be of quantitative importance in the time scale of the assay because von Bonsdorff et al. (1985) reported a linear degradation rate of 5% per h, when HRP was taken up by MDCK cells from the basolateral side. The amount of complex formed was quantitated using an ELISA described by Gruenberg et al. (1989). The assay had to be performed after internalization of avidin from the apical domain. When the conditions were reversed, namely avidin internalized basolaterally and bHRP apically, the large excess of avidin over bHRP within the cells (and to some extent also adsorbed nonspecifically to the polycarbonate filters) exceeded the capacity of the ELISA wells. Attempts made with biotinylated insulin as quencher (Braell, 1987) were unsuccessful, because it interfered with our ELISA assay, whereas bBSA did not.

Results

Confocal Microscopy of MDCK Cells

To visualize the organization of the endocytic pathways in filter-grown MDCK cells, the fluorescent fluid phase marker LY (Swanson et al., 1985) was selectively internalized from either the apical or the basolateral surface domain for various times at 37°C. The spatial distribution of the marker was analyzed by confocal beam scanning laser microscopy and the digitalized data were used to generate two- and three-dimensional views of the fluorescent specimens. Conventional fluorescence microscopy could not be used for imaging, because the MDCK cell layer is too thick and is grown on a filter that gives increased background fluorescence. These problems can be overcome by confocal microscopy. With this method it is possible to visualize sequentially a series of focal planes along the vertical axis of the MDCK cell, with each plane containing exclusively the fluorescence in focus. Fig. 1 shows 24 horizontal planes between the apical (plane *1*) and the basal poles (plane *24*), which document the complete cellular distribution of LY-labeled compartments after 5 min internalization from the basolateral side. Because the height of the cells in the layer varied, the tallest cells apparent in this field were in the lower left quadrant and the shortest in the upper left corner. The endosomes in these latter cells were first seen in plane *8*. In each cell, the endosomes appeared to distribute in a ring very close to the lateral membrane. When moving deeper into the monolayer, the endosomes surrounded the nucleus, which appeared as a black area in these images. These images show that the endosomes (labeled after 5 min of internalization) of two adjacent cells were distributed in double rows, each row lining the lateral membrane of one cell (see plane *13*). After specific labeling of the basolateral membrane (see below), these endosomes were observed to distribute not only along the lateral membrane (planes *1–2I*) in the typical ring-like pattern but also above the basal membrane facing the filter (planes *22* and *23*). This distribution suggests that internalization of fluid phase markers occurred equally from the entire basolateral membrane.

Spatial Organization of the Apical and Basolateral Endocytic Pathways

The presentation of the data was simplified by the selection of three representative planes in each subsequent focal series that illustrate the distribution of the fluid phase marker over the entire cell height (Fig. 2, *A* and *B*). The three focal planes were in the apical region of the cell (*I*), in the middle of the cell around the top of the nucleus (*II*), and in the most basal area of the cell (*III*). The nuclei were stained with propidium iodide (DNA-binding dye exhibiting a red fluorescence emission) after internalization of the endocytic markers and cell fixation, to provide an internal reference. Two consecutive focal series were then recorded to detect selectively either fluorophore, and superimposed plane to plane, using the image analysis program. In the resulting images,

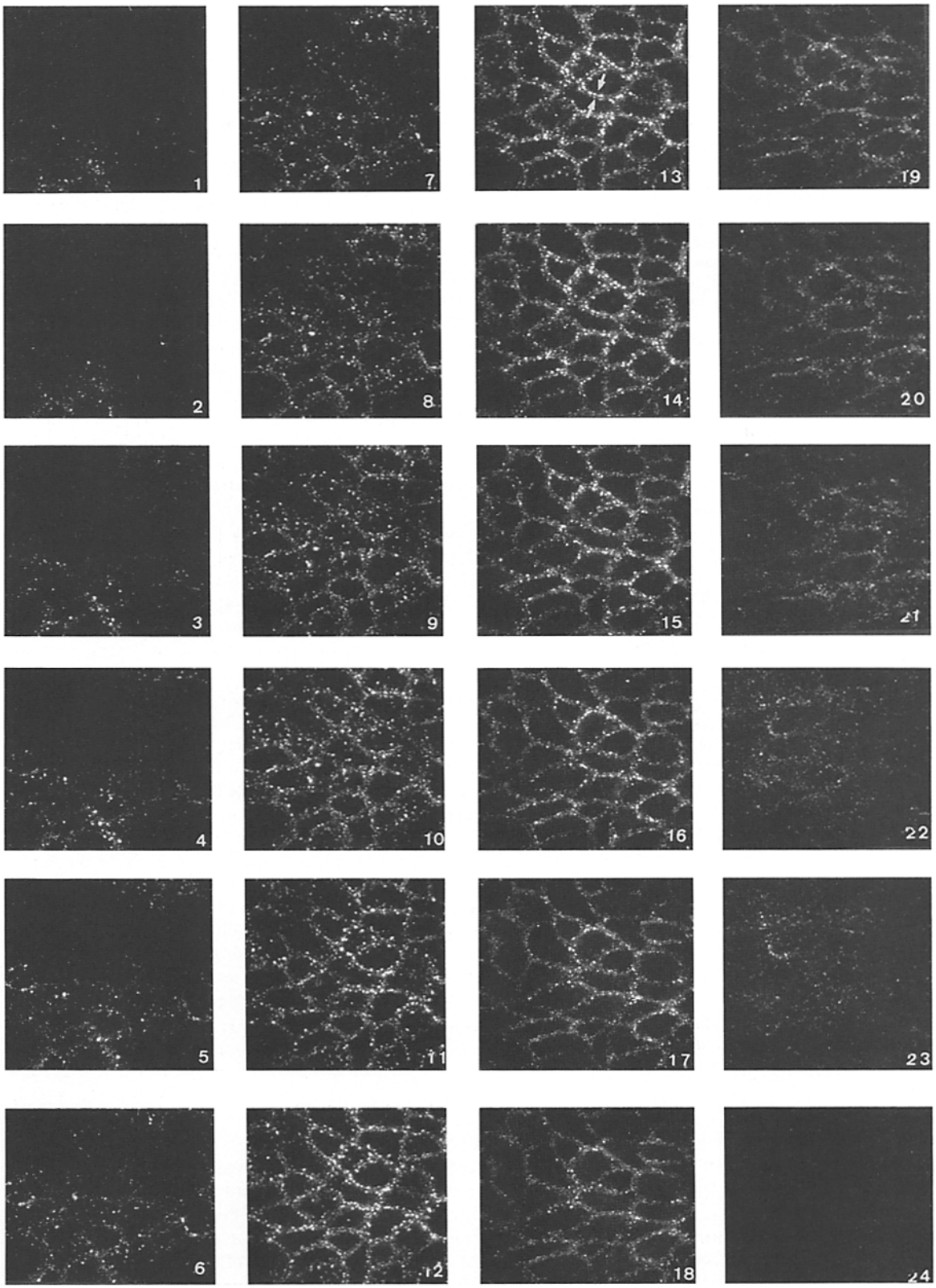

Figure 1. Confocal series showing the basolateral endosome distribution. LY was internalized for 5 min from the basolateral domain of the cell layer. Planes *1–24* are consecutive horizontal focal planes in a confocal series in which the cell layer was scanned along the vertical axis starting at the apical pole. The apical region of the cells above the tight junctions contained no labeling and is therefore not shown (above plane *1*). Plane *24* is an optical section in the filter next to the basal membrane and shows the background level of fluorescence of the filter. Because of differences in the height of the cells in the monolayer, the cells in the upper left and lower right quadrants come into focus later. Arrows in plane *13* show the endosome distribution of two adjacent cells as a double row, each lining the lateral membrane of one cell. Two consecutive sections are 0.5 μm apart and represents a field of 60 $\times$ 60 μm.

LY-labeled endosomes appeared in green (or yellow) and nuclei in red.

In Fig. 2 *B*, the three confocal planes document the distribution of basolateral endosomes after LY internalization; planes *I*, *II*, and *III* correspond respectively to planes *7*, *13*, and *22* in Fig. 1. After 5 min, LY labeled peripheral endosomes, and after 30 min of continuous basolateral internalization, the fluid phase marker also reached structures in the perinuclear area, which appeared heterogeneous in size and formed a punctate pattern above (*I*) and around the nucleus (*II* and *III*). When this 30-min internalization was followed by a 60-min chase in marker-free medium, most of the intracellular LY redistributed to the apical region and the peripheral rows of endosomes were no longer visible (*I* and *II*). The labeling in the basal part of the cell was significantly reduced (*III*).

When LY was internalized from the apical side for 5 min at 37°C, a fine punctate pattern depicting the peripheral endosomes was observed underneath the apical plasma membrane (Fig. 3 *A*). After 30 min of continuous apical internalization, LY appeared also in larger structures located mostly above the nucleus and to a lesser extent also around the lower part of the nucleus. A fine punctate pattern lining the lateral membrane became visible and may represent transcytotic vesicles en route to the basolateral side of the layer. The endocytic marker was depleted from the basal half of the cell during a subsequent 60-min chase in LY-free medium.

The digitalized data from the confocal analysis can be processed to generate stereo views of the whole cell layer. To provide spatial references within the cell, we first labeled the apical and the basolateral membrane and the nuclei using appropriate antibodies (stereo images, Fig. 3). The differences in cell height is shown by the wavy appearance of the apical membrane (Fig. 3, *top*). The basolateral membranes of the same cells are shown in Fig. 3 (*middle*). The nuclei occupied a large portion of the cell volume (Fig. 3, *bottom*).

We then generated stereo pair views (Fig. 4) to localize all the endocytic compartments labeled with LY relative to the basolateral membrane stained with WGA-Texas Red (*top*) or to the nuclei stained with propidium iodide (*middle* and *bottom*).

A comparison between the stereo pair images obtained after endocytosis from either cell surface domain showed that significantly less LY had accumulated in the cells after apical endocytosis (Fig. 4 *A*) than after basolateral endocytosis (Fig. 4 *B*). The different locations of the apical and basolateral endosomes in MDCK cells after 5 min of LY internalization were striking in these stereo images (*top*). We will refer to these endosomes underlying the apical and the basolateral plasma membrane domains as apical and basolateral early endosomes, respectively (see Courtoy, 1989; Gruenberg et al., 1989). Their spatial location is distinctly peripheral and they seem to contain the bulk of the endocytosed label up to 10 min of internalization (data not shown).

The stereo views after 30 min of LY internalization became complex. In addition to the early endosomes, perinuclear structures were labeled from both sides (*middle*). A significant amount of the internalized LY (particularly after apical application) was released during the subsequent 60-min chase in marker-free medium (*bottom*). The retained LY was mostly confined to the apical perinuclear region after both apical and basolateral internalization. The perinuclear endocytic structures seen after longer internalization (>20 min) most likely correspond to late endosomes and lysosomes (see Courtoy, 1989; Gruenberg and Howell, 1989).

Biochemical Quantitation of Endocytosis and Transcytosis

We proceeded to correlate the spatial distribution of the apical and basolateral endocytic elements with a kinetic analysis of both pathways. HRP was used as a fluid phase marker and was administered either apically or basolaterally to the cell monolayer. We determined the amount of HRP accumulated in the cell after different times of continuous internalization at 37°C, as well as the net amount of HRP transcytosed across the cell layer in both directions (Fig. 5). As observed previously (von Bonsdorff et al., 1985), the extent of endocytosis from the apical side was strikingly lower than from the basolateral side; 30 times less HRP was intracellular after 60 min of internalization. The amount of intracellular HRP retained after basolateral application, reached a plateau between 10 and 20 min and subsequently started to increase linearly. These kinetics may reflect a rapid filling of the early endosomes (0–10 min) followed by an apparent steady state (10–20 min) between HRP internalization and efflux by recycling and transcytosis before significant amounts of HRP are delivered to late endocytic compartments (>20 min). This plateau was also seen after apical endocytosis but it was not so pronounced. In agreement with von Bonsdorff et al. (1985), we found that the amounts of fluid transcytosed in both apical and basolateral directions were of the same magnitude.

Biochemical Quantitation of Recycling

The third route, namely the recycling of endocytosed fluid, could not be monitored during continuous HRP internalization. To quantitate the extent of recycling, cells were first preloaded for different times at 37°C from either the apical or the basolateral side, washed extensively at 4°C to remove surface adsorbed HRP and then reincubated in marker-free medium for various times at 37°C. The kinetics of recycling were determined by measuring the amount of HRP released into the medium bathing the surface from whence internalization had occurred. The kinetics of HRP transcytosed and retained inside the cell were also determined.

After internalization of HRP for 60 min from the basolateral side, followed by a 90-min chase in marker-free medium, 10% of the internalized HRP was recycled back to the basolateral medium and 10% was transcytosed, corresponding to a total efflux of 20% (Fig. 6 *B*). In contrast, when the same experiment was carried out from the apical side (Fig. 6 *A*), the total efflux corresponded to 70% of the internalized HRP with 30% recycled back to the apical side and 40% transcytosed to the basolateral medium. Neither recycling nor transcytosis was detected when the chase was carried out at 4°C in marker-free medium (data not shown). These results suggest that the bulk of HRP internalized during 1 h from the basolateral side was transferred to late endocytic compartments from where little if any was recycled or transcytosed. In contrast, when internalized from the apical side for the same period of time, the bulk of HRP was released from the cell layer equally by recycling and transcytosis. Ap-

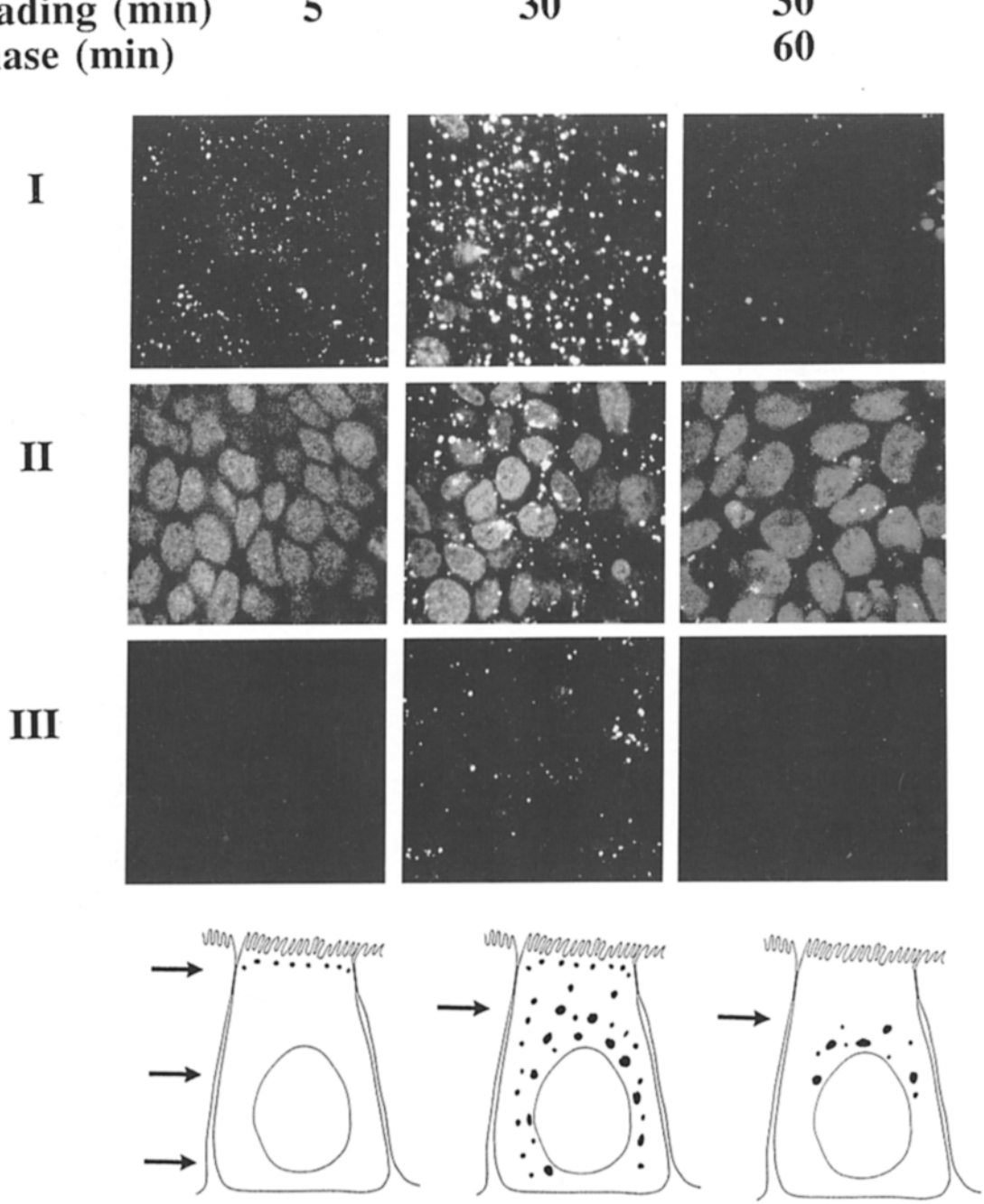

Figure 2. Distribution of apical and basolateral endocytic compartments in the apical, middle, and basal region of MDCK cells. LY was internalized at 37°C from the apical (*this page*) or the basolateral (*next page*) side of the cells for 5, 30, or 30 min followed by 60 min incubation in marker-free medium. After fixation of the cells, the nuclei were labeled with propidium iodide. The LY and the propidium iodide fluorescence of the specimens were observed sequentially in the confocal microscope. Then, the corresponding focal planes of each series were superimposed in a double-colored image in which the LY endosomal pattern appeared in green (or yellow) and the propidium iodide nuclear pattern appeared in red. The figure is reproduced in black and white. The LY staining can be differentiated from the nuclear staining by its dot appearance. A schematic outline of the endosomal pattern is represented for each observed time point and the level of the three selected planes indicated by arrows. On this page, note that after 5 min, plane *I* is located closer to the apical surface than the corresponding planes to visualize the distribution of apical early endosomes. Appearance of some nuclei in plane *I* reflects differences in cell height (see Fig. 1). Each image represents a field of 60 × 60 μm^2.

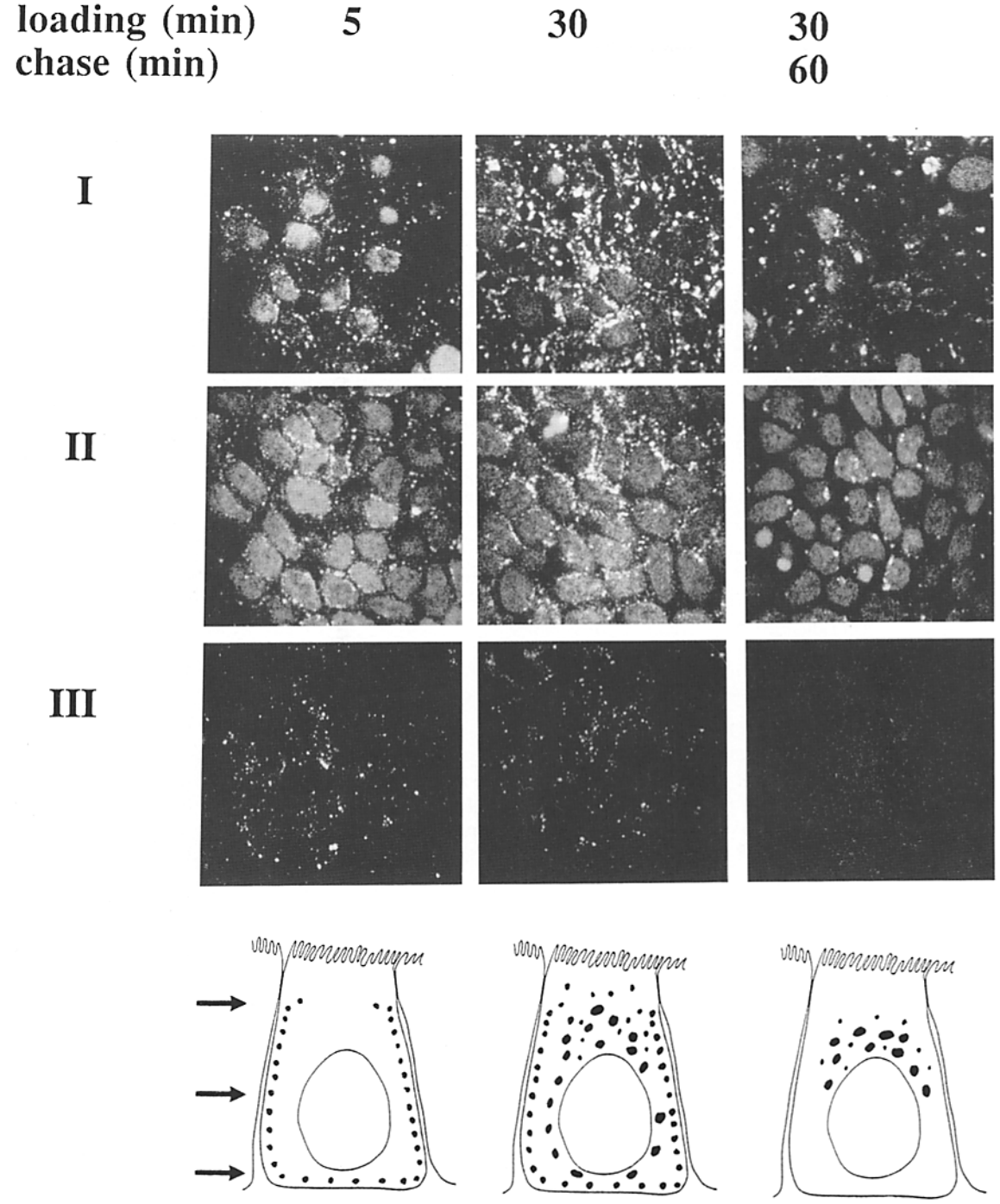

Figure 2.

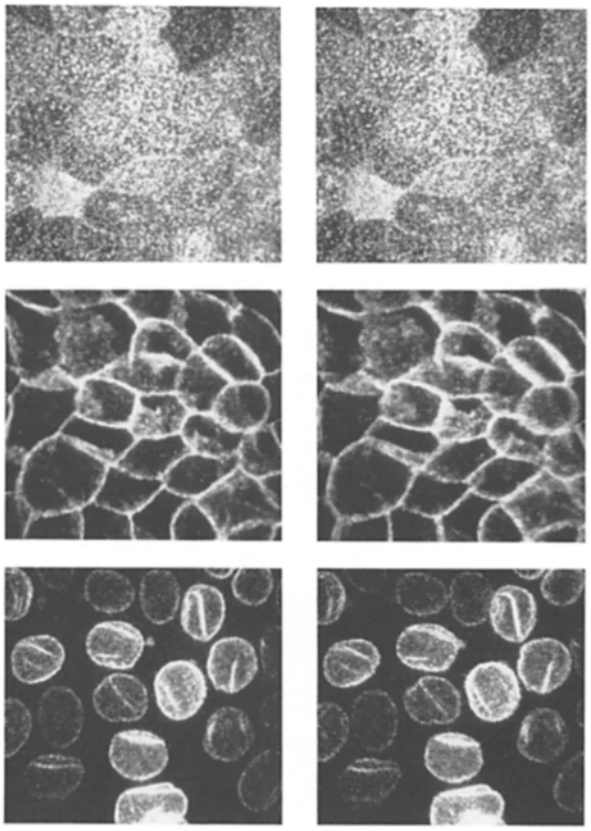

Figure 3. Three-dimensional organization of MDCK cells. Stereo-paired images of cells labeled with mAbs against: the apical 114-kD protein (*top*) the basolateral uvomorulin (*middle*); and the nuclear lamin B (*bottom*). The distributions of specific antibodies were revealed, using a second antibody against mouse IgG coupled either to rhodamine, Texas Red, or fluorescein. Series of 23–30 focal planes from the apical to the basal pole of the cell (two consecutive planes were 0.5 μm apart) was recorded in the confocal microscope (as in Fig. 1) and a pair of stereo pictures was generated. Each stereo image is an extended focus of all the planes, recorded in the confocal series. The angle between the left and the right stereo images is obtained by a shift of one pixel along the x-axis. (*Top* and *middle*) The same cells are shown with labeling delineating the apical and the basolateral membrane, respectively. The images show fields of 60 × 60 μm.

parently, little HRP had been transferred to later stages of the apical endocytic pathway.

The Internalized Fluid Is Recycled and Transcytosed from Early Endosomes

To characterize more precisely the kinetics of recycling and transcytosis, MDCK cell layers were loaded for short times to fill only the early endosomes with HRP. When basolateral endosomes were preloaded for 5, 10, or 15 min, subsequent recycling and transcytosis followed a similar time course (Fig. 7 *B*). After 30 min efflux, approximately equal amounts of HRP were delivered to the apical and the basolateral medium by transcytosis and recycling, respectively, and these amounts stayed constant irrespective of the loading period. The main change observed when the loading period was extended from 5 to 15 min was that of the fraction of HRP remaining inside the cell after a 30-min chase in HRP free-medium increased from 40 to 65%.

When the same protocol was applied to the apical side, different results were obtained (Fig. 7 *A*). After preloading the apical early endosome for 5 min, a rapid and extensive recycling to the apical medium was observed, but transcytosis to the basolateral medium was only detected after a lag of 10 min and this lag time was still observed when early apical endosomes had been loaded for 10 min. By the end of the chase in HRP-free medium, the amount of HRP that had been transcytosed equaled the amount recycled. The amount that was retained in the cells was only ~30% of the HRP that had been internalized during the 15-min loading period.

In Fig. 8, we have plotted the time course of HRP uptake by the cell layer (*solid symbols*) compared with the total efflux (sum of recycling and transcytosis; *open symbols*) at the corresponding times. The fast initial rate of HRP efflux at all time points of apical endocytosis shows the rapid depletion of apical endosomal fluid content (Fig. 8 *A*). In contrast, the much smaller HRP efflux during basolateral endocytosis suggests that the bulk of internalized HRP is routed to late endocytic compartments, where recycling and transcytosis cannot occur (Fig. 8 *B*). In Table I, the data for fluid recycling, transcytosis, and retention within the cell have been summarized.

Convergence of the Apical and the Basolateral Endocytic Pathways

Confocal microscopy analysis showed that the fluid phase marker entered late endocytic structures, located all around the nucleus ~30 min after internalization from either side of the cell layer and that an additional hour of incubation in marker-free medium led to accumulation of the marker in the region above the nucleus. Therefore, we analyzed whether mixing of apical and basolateral endocytic markers occurred in these structures.

Two different fluid phase markers, dextran-Texas Red and LY were applied simultaneously to opposite sides of the cell layer. As expected, dextran-Texas Red and LY were first observed in the two distinct groups of early endosomes after 5 min of internalization at 37°C (data not shown). After 15 min of incubation at 37°C, a colocalization of both markers became apparent in structures above the nucleus (data not shown). After 30 min, this colocalization extended to structures located in the more basal region of the cells (Fig. 9 *A*). When the cell layers were incubated for an additional hour in marker-free medium after a 30-min loading period, many endocytic structures containing both markers were observed. These endocytic elements where meeting of the two pathways occurred were located mainly around the apical part of the nucleus, whereas the basal half was depleted of markers (Fig. 9 *B*).

Quantitation of the Meeting

The extent of this meeting was quantitated using a biochemical assay based on the high affinity of avidin for biotin that has been useful for studies of endocytic vesicle fusion in vitro (Braell, 1987; Gruenberg et al., 1989). Avidin was applied apically and bHRP was applied basolaterally. After different times of internalization, the endocytic compartment of MDCK cells contained either avidin, bHRP, or both. The

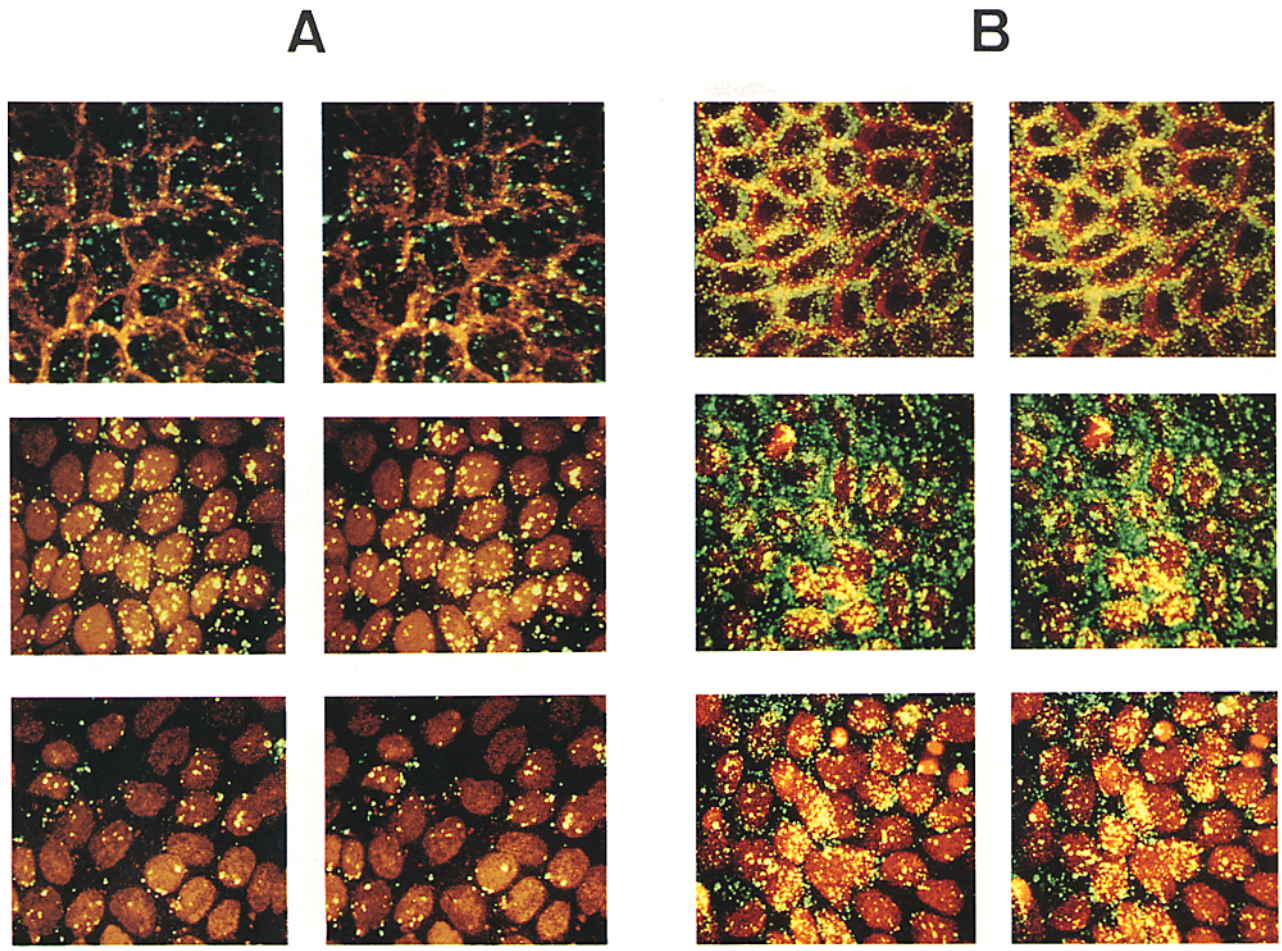

Figure 4. Stereo pair images of apical and basolateral endocytic compartments. LY was internalized at 37°C from the apical (*A*) or the basolateral (*B*) side of the cells for 5 (*top*), 30 (*middle*), or 30 min followed by 60 min incubation in marker-free medium (*bottom*). After 5 min of internalization, the basolateral plasma membrane was labeled with WGA-Texas Red. At the late time points, the nuclei were labeled after fixation of the cells with propidium iodide. Stereo pair images were generated as described in Fig. 3. The endosomal pattern appears in green (or yellow) whereas basolateral plasma membrane or nuclei appear in red. Each image represents a field of 60 × 60 μm^2.

formation of the avidin-bHRP complex would only occur when the two pathways had met and mixed their contents in vivo. The amount of avidin-bHRP complex formed in vivo was quantitated after solubilization of the cells in the presence of bBSA to quench the free avidin that had been endocytosed but did not react with bHRP during internalization. The relative efficiency of the meeting could be quantitated as the percentage of the total avidin internalized from the apical

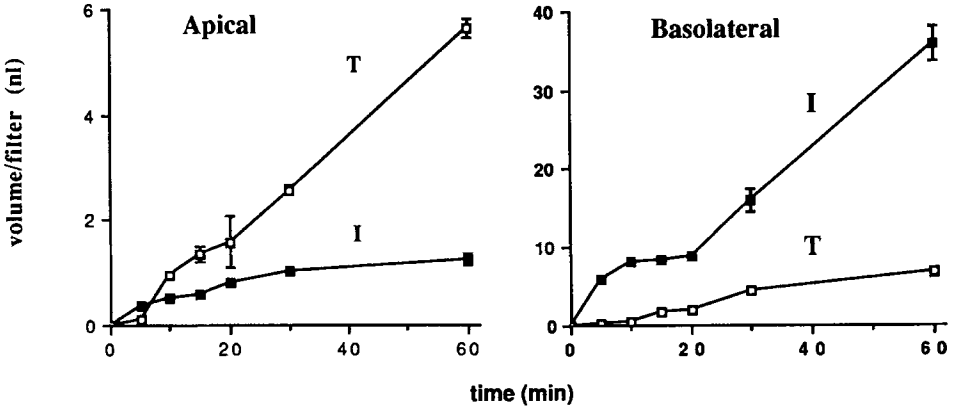

Figure 5. Polar uptake and transcytosis of HRP. After incubation at 37°C in the presence of HRP for the indicated times, the medium opposite the side of internalization was collected and the monolayer washed at 4°C and extracted. The enzymatic activity of HRP in the media and cell extracts were converted into the corresponding volume of fluid using the specific activity of HRP in the medium at the start of the uptake. Each point on the graph represents the mean of at least four filters processed during two different experiments and the bar is the SEM when larger than the size of the symbol. (*Left*) Amount of HRP retained intracellular (*I, closed symbols*) and transcytosis (*T, open symbols*) from the apical side. (*Right*) Amount of HRP retained intracellular (*I, closed symbols*) and transcytosis (*T, open symbols*) from the basolateral side.

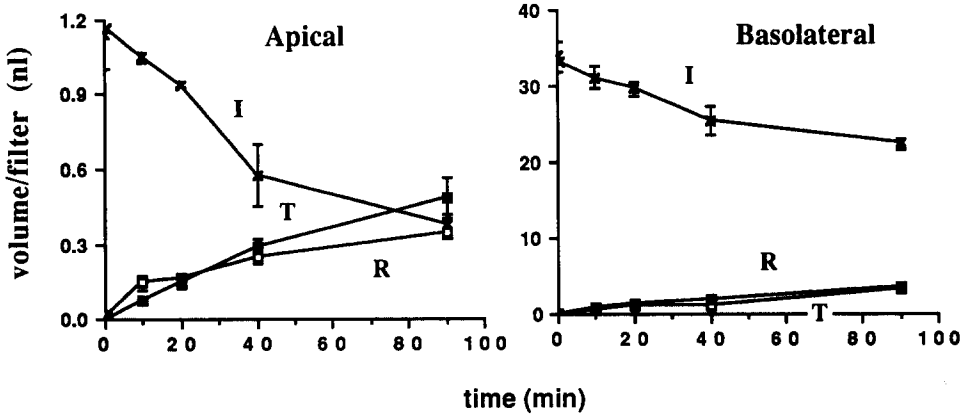

Figure 6. Recycling and transcytosis of preinternalized HRP. Cells were preloaded at 37°C for 60 min with HRP on the apical or the basolateral side of the monolayer. After washing at 4°C, the cell layers were reincubated in marker-free medium at 37°C. At the indicated times, both apical and basolateral medium were collected, the cells were washed at 4°C and extracted. The HRP activity in the sample was converted into volume as in Fig. 5 and plotted versus the time of reincubation in HRP-free medium. (*Left*) Apical preloading. HRP activity remaining in the cell (*I*, *crosses*). HRP recycled to the basolateral medium (*R*, *open symbols*). HRP transcytosed to the apical medium (*T*, *closed symbols*). (*Right*) Basolateral preloading. HRP activity remaining in the cell (*I*, *crosses*). HRP recycled to the apical medium (*R*, *open symbols*). HRP transcytosed to the basolateral medium (*T*, *closed symbols*). Error bars are shown as in Fig. 5.

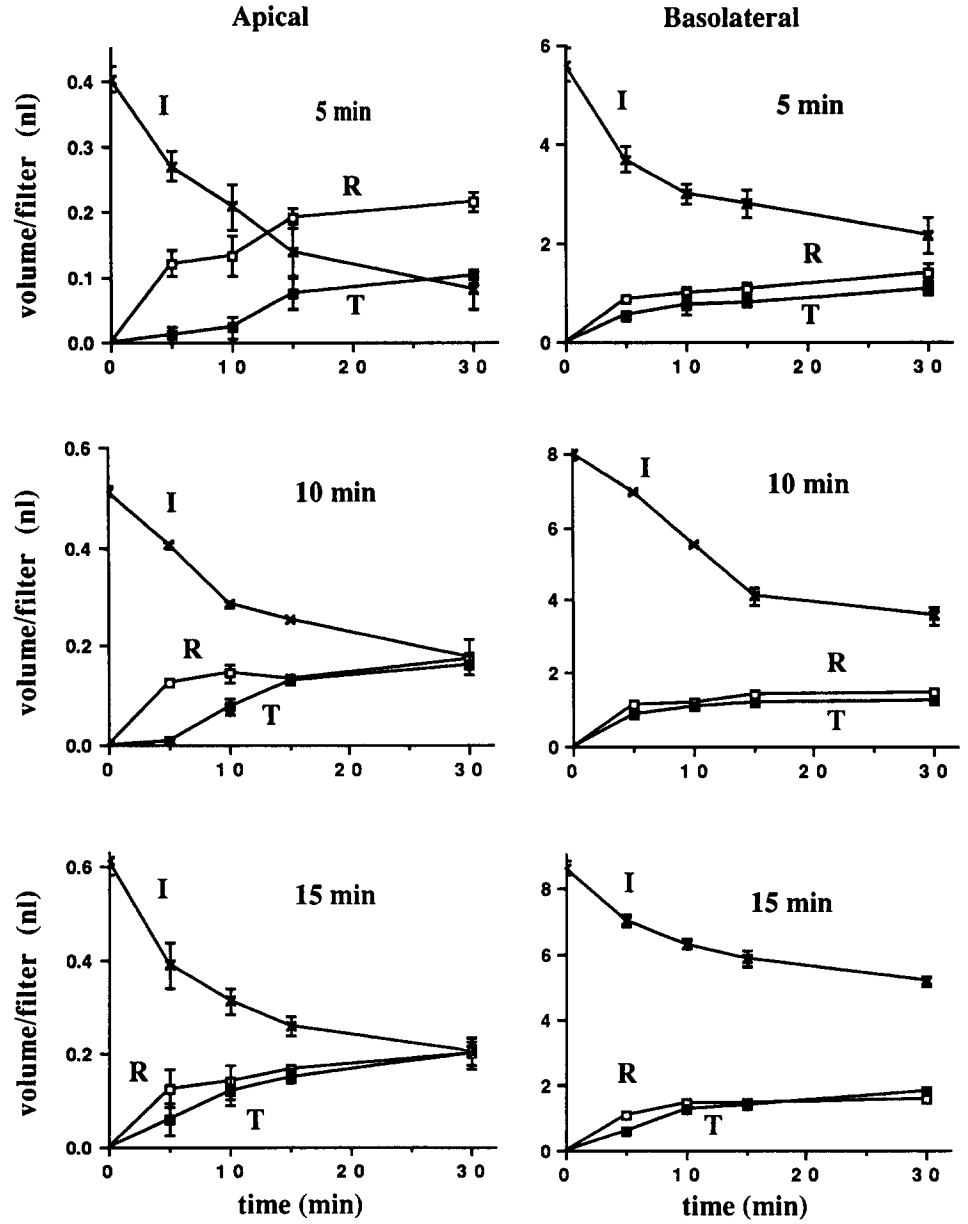

Figure 7. Kinetics of HRP efflux (recycling and transcytosis) from apical and basolateral early endosomes. HRP was applied to the apical (*left*) and the basolateral (*right*) side of the monolayer for 5, 10, or 15 min at 37°C. Then, HRP efflux was followed in marker-free medium as in Fig. 6. Symbols are as shown in Fig. 6 and error bars are as shown in Fig. 5.

Table I. Rate of Fluid Phase Marker Recycling, Transcytosis, and Intracellular Accumulation by Filter-grown MDCK Cells

	Side of Internalization	
	Apical	Basolateral
	10^{-3} μm^3/min per cell	
Reycling	27.5	30
Transcytosis	27.0	28
Intracellular accumulation	5.5	160
Endocytosis	60	218

Transcytosis and intracellular accumulation rates were calculated from the values obtained after 60 min of continuous uptake from either the apical or the basolateral side of the cell layer. These values were from Fig. 5 and converted to μm^3/cell per min using 3.75×10^6 cells/filter as determined in the companion paper (Parton et al., 1989). Because recycling could not be measured during continuous internalization experiments, the fraction of internalized marker recycled to either surface domain was calculated from the experiments described in Fig. 7, *A* and *B*. The recycling rate was calculated relative to that of transcytosis, assuming that transcytosis and recycling take place from the early endosomes. The ratio of the amount recycled and transcytosed after loading for 15 min and subsequent incubation in HRP-free medium for 30 min, should give a realistic estimate of the rates. The endocytosis rate was calculated as the sum of the three rates; recycling, transcytosis, and intracellular accumulation.

side that had formed the avidin-bHRP complex intracellularly during the experiment. The total amount of internalized avidin was determined after solubilization in the absence of bBSA. It could be argued that a fraction of either marker was transcytosed, bound its partner outside the cell and was then reinternalized, contributing to the observed signal. However, this is unlikely as the transcytosed marker would be considerably diluted (see Table I; maximally 0.2–0.5% of the concentration at the opposite side of the cell layer). Furthermore, no avidin could be detected by immunocytochemistry at the basolateral membrane after our washing procedure (not shown).

At 37°C, the in vivo formation of avidin-bHRP complexes was first detected after 15 min internalization. After 60 min internalization of the two markers, 20% of the avidin had met bHRP (Fig. 10, *a* and *b*). The formation of the complex was greatly reduced at 20°C (Fig. 10 *c*). The lag time of 15 min at 37°C, as well as the reduced signal at 20°C (Griffiths et al., 1988; Gruenberg et al., 1989) suggested that the two pathways met in a late endocytic compartment. The percentage of meeting was increased to 50% when internalization of both markers was carried out for 15 min followed by a subsequent chase for an additional 60 min in marker-free medium at the apical side (Fig. 10 *c*). The time-course of complex formation agreed well with the confocal microscopy analysis (Fig. 9) and confirmed that the convergence of the two endocytic pathways occurred in late endocytic compartments.

Discussion

In this study, the general organization of the apical and basolateral endocytic pathways has been visualized in MDCK cells by the use of confocal microscopy and three-dimensional image reconstruction. We have complemented this morphological characterization by a detailed analysis of how the fluid phase marker, HRP, is handled by the polarized cell after internalization from either side of the cell layer. Our results demonstrate that there are distinct sets of early apical and basolateral endosomes where recycling and transcytosis primarily occur.

The early endosomes are seen close to the plasma membrane domain to which the fluid phase marker had been applied. Apical early endosomes are distributed below the apical microvilli above the ring of tight junctions (Bomsel, M., unpublished observation), whereas basolateral early endosomes lie alongside the lateral as well as the basal membrane. The peripheral location of early endosomes conforms with earlier observations in nonpolarized cells (Herman and Albertini, 1981; Pastan and Willingham, 1981) as well as in hepatocytes (Wall et al., 1980; Geuze et al., 1983; Hopkins, 1983), kidney proximal tubules (van Deurs and Christensen, 1984; Rodman, 1986), exocrine acinar cells (Oliver and Hand, 1978; Oliver, 1982) and enterocytes (Gonnella and Neutra, 1984). Further work is required to analyze the early endosomes biochemically and to find out whether they conform to the criteria defined for early endosomes in other cell types (Wolkoff et al., 1984; Mueller and Hubbard, 1986; Schmid et al., 1988; Cain et al., 1989; Fuchs et al., 1989; Gruenberg et al., 1989). The distinct spatial distribution of apical and basolateral early endosomes in MDCK cells clearly suggests that each population is exclusively involved

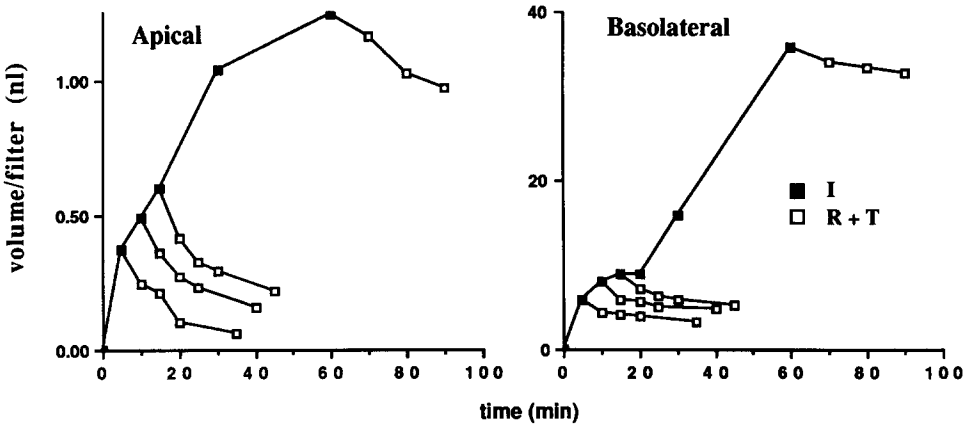

Figure 8. Kinetics of HRP retention and efflux in the MDCK cell layer after endocytosis from either surface domain. (*Left*) After apical internalization of HRP. (*Right*) After basolateral internalization of HRP. Intracellular HRP was as measured in Fig. 5 (*I, solid symbols*). HRP efflux was determined after the indicated period of preloading and further incubation in marker-free medium. Efflux was calculated as the sum of the HRP recycled and transcytosed (see Figs. 6, 7, and 8). *R+T, open symbols.*

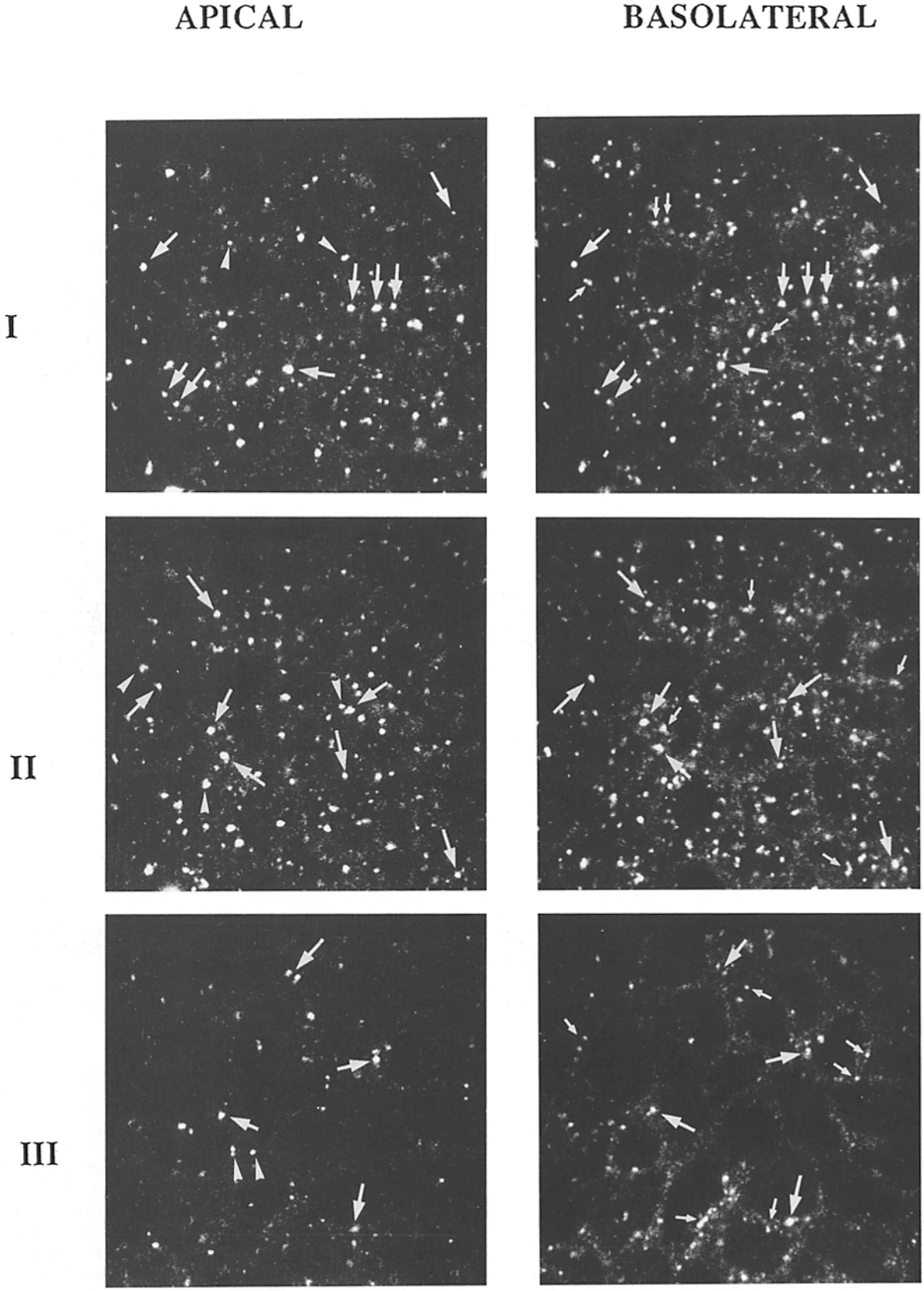

Figure 9. Meeting of the apical and basolateral endocytic pathways. Texas Red-dextran (*left*) and LY (*right*) were applied for 1 h at 37°C (*this page*) to the apical and basolateral sides of the monolayer, respectively, followed by a 30-min incubation in marker-free medium (*next page*). The samples were scanned twice to generate confocal series, each with the appropriate filters. The overlapping between the Texas Red-dextran and LY patterns was analyzed plane to plane to identify the endocytic compartments containing both markers. The three planes presented are located at the same heights of the cell, as in Fig. 2. Examples of compartments, labeled with both markers (*large arrows*), Texas Red-dextran only (*arrowheads*), or LY only (*small arrows*), are pointed out. Note that on next page, the basal half of the cell (planes *III*) is depleted of labeled structures.

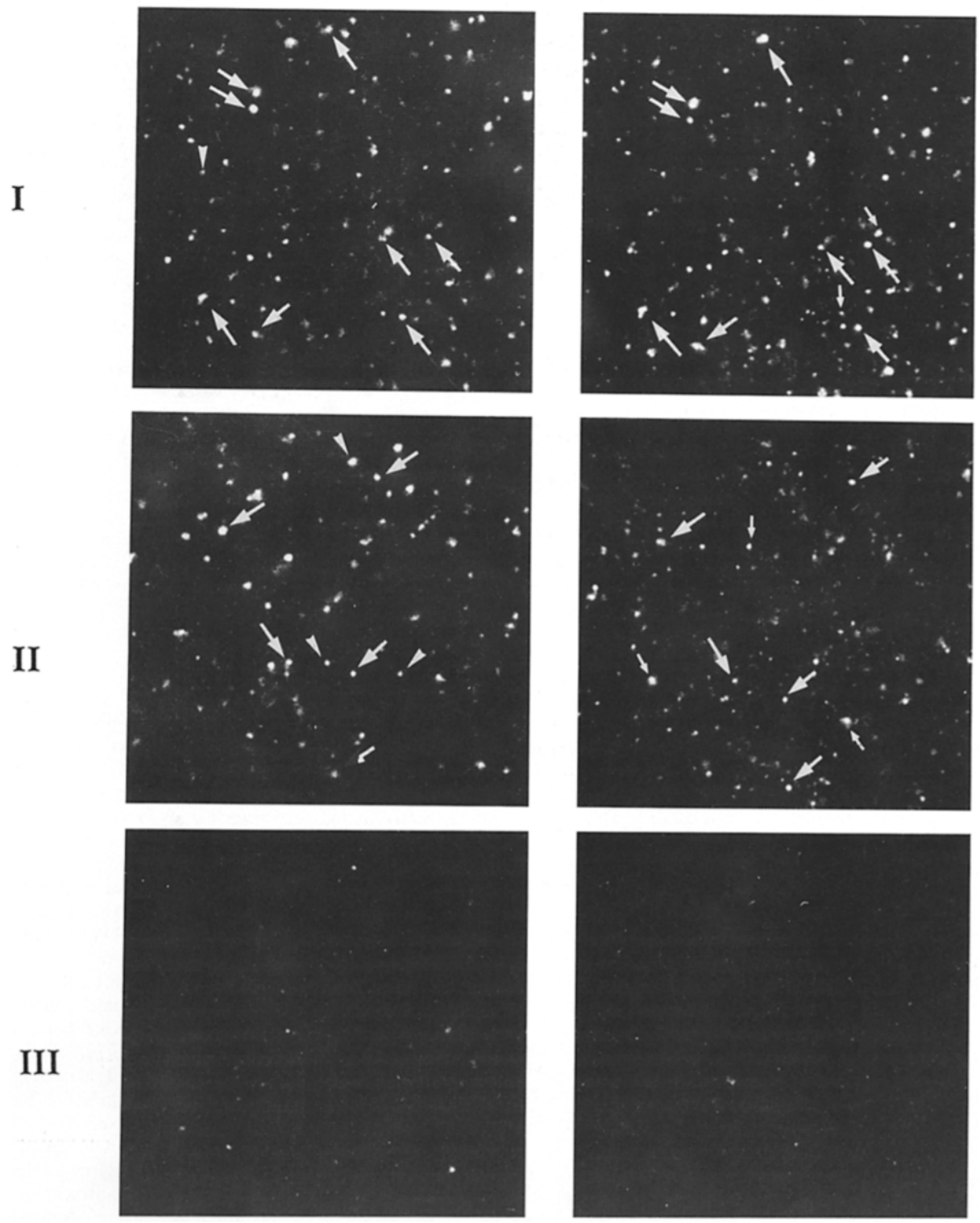

Figure 9.

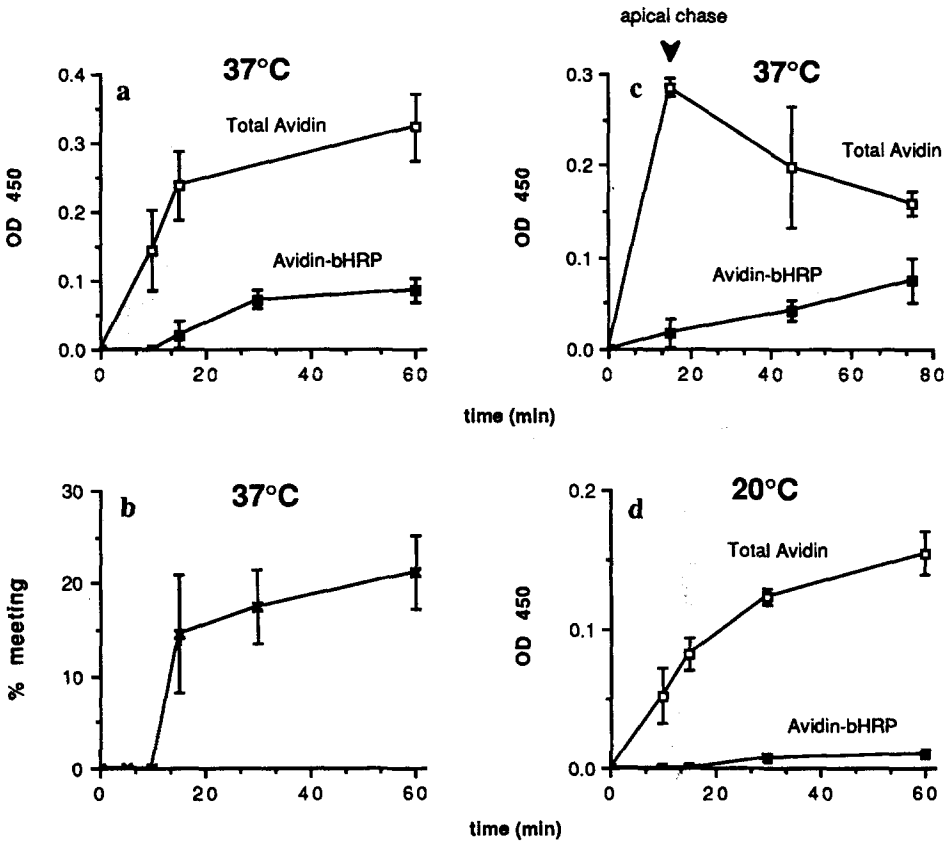

Figure 10. Time course and extent of the meeting of the apical and basolateral endocytic pathways. The meeting assay was carried out with avidin and bHRP internalized from the apical and the basolateral sides of filter-grown MDCK cells, respectively. Cells were solubilized (*a*) in the presence of bBSA (*closed symbols*) to quantify the amount of avidin-bHRP complex found in vivo during the internalization period or (*b*) in the absence of bBSA (*open symbols*) to quantify the total amount of avidin internalized apically during the same period of time. The ODs of the HRP enzymatic activity of the sample measured in the ELISA assay are plotted versus the time of internalization of the two markers. SD (*bars*) are calculated from four sets of triplicate experiments. (*a*) Time course of the meeting assay where internalization of the markers was continous at 37°C. (*b*) The values in *a* are expressed as percent of avidin endocytosed from the apical side that has met bHRP endocytosed from the basolateral side (*crosses*). (*c*) The meeting assay was carried out with avidin internalized at 37°C for 15 min and then chased for 30 or 60 min, whereas bHRP was continuously internalized from the basolateral side. The arrow indicates the time (15 min) when the apical medium containing avidin was replaced with marker-free medium to chase the avidin into late endocytic compartments. (*d*) Time course of the meeting assay at 20°C.

in endocytosis from the corresponding plasma membrane domain. This is supported by our confocal and biochemical observations that two different fluid phase markers internalized simultaneously from either side of the cell layer do not colocalize in early endosomes but meet at a later stage of the pathway.

The analysis of the kinetics of fluid phase marker internalization, recycling, transcytosis, and intracellular retention reveals important characteristics of membrane traffic to and from early endosomes at either surface domain. The total amount of fluid phase marker internalized appears 3.6 times higher at the basolateral surface than at the apical surface. However, because the ratio of apical to basolateral plasma membrane surface area in filter-grown MDCK strain I cells is 3.8 (Parton et al., 1989), our conclusion is that the amount of fluid internalized per unit of plasma membrane surface area is similar from both domains, corresponding to $\sim 1.2 \times 10^{-4}$ μm^3/min, in keeping with our earlier proposal (von Bonsdorff et al., 1985).

Although fluid was internalized at the same rates from both surface domains per unit area, apical and basolateral early endosomes distributed their fluid phase content for recycling, transcytosis, or towards later endocytic compartments with strikingly different kinetics. 5–15 min after apical internalization, the efflux (recycling and transcytosis) was ninefold higher than the efflux after basolateral internalization. Correspondingly, the fraction of basolaterally internalized HRP that accumulated intracellularly was nine times higher than measured from the apical side. These results suggest that the content of basolateral early endosomes is far more efficiently routed to perinuclear endocytic compartments than returned to the medium by recycling or transcytosis. In contrast, most of the content of apical early endosomes is recycled or transcytosed. This agrees well with morphological observations in intercalated kidney cells showing that efficient apical recycling occurred but that little HRP internalized from the apical side was observed in structures deep in the cytoplasm (Brown, 1989). Efficient recycling from the apical early endosome to the apical domain has also been reported in proximal tubules (Christensen, 1982; van Deurs and Christensen, 1984; Hatae et al., 1988).

The kinetic studies show that the half-time of fluid content recycling from the early endosomes was ~5 min both after apical and basolateral internalization. Rapid recycling of fluid phase markers from the early endosome with similar kinetics has also been observed in several nonpolarized cells (Besterman et al., 1981; Adams et al., 1982; Swanson et al., 1985). Transcytosis of early endosomal content occurred with a similar half-time from the apical and from the basolateral side, corresponding to a value of ~10 min. This somewhat larger half-time when compared with recycling presumably reflects the slower transport of transcytotic vesicles

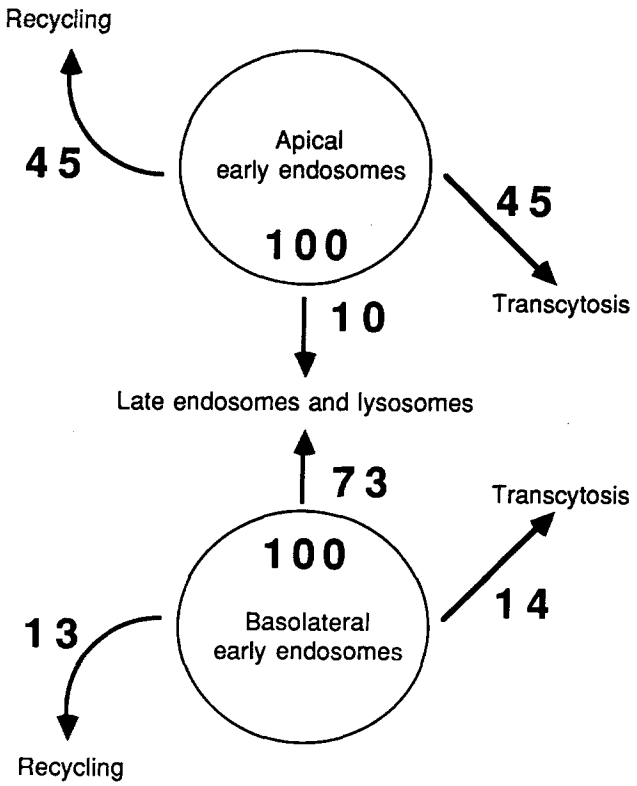

Figure 11. The distribution of fluid content from the apical and basolateral early endosomes for recycling, transcytosis, and transport to late endocytic compartments. The values shown in this schematic illustration are taken from Table I. As discussed in the text, the amount of HRP internalized from the basolateral side was 3.6 times higher than from the apical side.

from the early endosome, underlying the plasma membrane from which endocytosis occurred, to the opposite membrane domain.

Our observations on the routing of early endosomal content from the apical or the basolateral side are summarized in Fig. 11. The amounts of fluid phase marker internalized apically and basolaterally are in a ratio of 3.6, which is not only similar to the ratios of plasma membrane domains but also to the ratios of early endosomal volumes (Parton et al., 1989). Thus, 100 molecules of solute internalized from one unit of basolateral plasma membrane surface area distributed within the same early endosomal volume as 100 molecules internalized from one unit of apical plasma membrane surface area. As a consequence, the subsequent redistribution of solutes present in early endosomes becomes directly comparable for both pathways. Of the solute molecules that have entered basolateral early endosomes, 73% are routed to late endocytic compartments, whereas 13% are recycled and 14% are transcytosed. In contrast, the apical early endosomes distribute only 10% of their content to late endocytic compartments. The other 90% is released from the cell in equal amounts by recycling and transcytosis. These values suggest important differences in membrane traffic from the early apical and basolateral endosomes, are are likely to reflect functional characteristics of each pathway. It will be interesting to see how these characteristics differ in other epithelial cell types.

Simultaneous internalization of two different markers from either side of the cell layer shows that the two pathways start to converge after 15 min of endocytosis in the perinuclear region. This was shown both by confocal microscopy and by direct biochemical analysis. In the companion paper (Parton et al., 1989), the characterization of the compartments where the two apical and basolateral pathways meet has been extended to the ultrastructural level.

The authors thank E. Stelzer, R. Pick, C. Storz, and R. Stricker for their assistance during the confocal microscopic studies. Without their efforts this study would not have been possible. We are grateful to Hilkka Virta for help with cell cultures; to B. Mairs and the European Molecular Biology Laboratory (EMBL) photographic section for advice and excellent photographic work; to G. Griffiths, K. E. Howell, and C. Butor for fruitful discussions throughout this work; and to A. Wandinger-Ness for careful reading of the manuscript. The nucleopore filters (Transwell) were kindly provided by H. Lane (Costar Corp., Cambridge, MA).

M. Bomsel was a recipient of a long-term European Molecular Biology Organization (EMBO) fellowship; K. Prydz was a recipient of a long-term fellowship from the National Council of Science and Humanities, Norway (NAVF); and R. Parton was a recipient of a long-term Royal Society and an EMBO fellowship.

Received for publication 16 June 1989 and in revised form 18 September 1989.

References

Abrahamson, D. R., and R. Rodewald. 1981. Evidence for the sorting of endocytic vesicle contents during the receptor-mediated transport of IgG across the newborn rat intestine. *J. Cell Biol.* 91:270–280.

Adams, C. J., K. M. Maurey, and B. Storrie. 1982. Exocytosis of pinocytic contents by chinese hamster ovary cells. *J. Cell Biol.* 93:632–637.

Balcarova-Ständer, J., S. E. Pfeiffer, S. D. Fuller, and K. Simons. 1984. Development of cell surface polarity in the epithelial Madin-Darby canine kidney (MDCK) cell line. *EMBO (Eur. Mol. Biol. Organ.) J.* 3:2687–2694.

Berod, A., B. K. Hartmann, and J. F. Pujol. 1981. Use of formaldehyde solutions at variable pH for the localization of tyrosin hydroxylase. *J. Histochem. Cytochem.* 29:844–850.

Besterman, J. M., J. A. Airhart, R. C. Woodworth, and R. B. Low. 1981. Exocytosis of pinocytosed fluid in cultured cells: kinetic evidence for rapid turnover and compartmentation. *J. Cell Biol.* 91:716–727.

Braell, W. A. 1987. Fusion between endocytic vesicles in a cell-free system. *Proc. Natl. Acad. Sci. USA.* 84:1137–1141.

Brown, D. 1989. Vesicle recycling and cell-specific function in kidney epithelial cells. *Annu. Rev. Physiol.* 51:771–784.

Cain, C. C., D. M. Sipe, and R. F. Murphy. 1989. Regulation of endocytic pH by the Na^+,K^+-ATP-ase in living cells. *Proc. Natl. Acad. Sci. USA.* 86:544–548.

Christensen, E. I. 1982. Rapid membrane recycling in renal proximal tubule cells. *Eur. J. Cell Biol.* 29:43–49.

Courtoy, P. 1989. Dissection of endosomes. *In* Intracellular Trafficking of Proteins. C. Steer and J. Ciechanover, editors. Cambridge University Press, New York. In press.

Fuchs, R., S. Schmid, and I. Mellman. 1989. A possible role for sodium potassium-ATPase in regulating ATP-dependent endosome acidification. *Proc. Natl. Acad. Sci. USA.* 86:539–543.

Fuller, S., C.-H. von Bonsdorff, and K. Simons. 1984. Vesicular stomatitis virus infects and matures only through the basolateral surface of polarized epithelial cell line, MDCK. *Cell.* 38:65–77.

Geuze, H. J., J. W. Slot, G. J. A. M. Strous, H. F. Lodish, and A. L. Schwartz. 1983. Intracellular site of asialoglycoprotein receptor-ligand uncoupling: double-label immunoelectron microscopy during receptor-mediated endocytosis. *Cell.* 32:277–287.

Gonnella, P. A., and M. R. Neutra. 1984. Membrane-bound and fluid-phase macromolecules enter separate prelysosomal compartments in absorptive cells of suckling rat ileum. *J. Cell Biol.* 99:909–917.

Griffiths, G., B. Hoflack, K. Simons, I. Mellman, and S. Kornfeld. 1988. The mannose-6-phosphate receptor and the biogenesis of lysosomes. *Cell.* 52:329–341.

Gruenberg, J., G. Griffiths, and K. E. Howell. 1989*a*. Characterization of the early endosome and putative endocytic carrier vesicles in vivo and with an assay of vesicle fusion in vitro. *J. Cell Biol.* 108:1301–1316.

Gruenberg, J., G. Griffiths, and K. E. Howell. 1989*b*. Membrane traffic in endocytosis. *Annu. Rev. Cell Biol.* In press.

Gumbiner, B. 1987. Structure, biochemistry, and assembly of epithelial tight junctions. *Am. J. Physiol.* 5922:C749–758.

Gumbiner, B., and K. Simons. 1986. A functional assay for proteins involved

in establishing an epithelial occluding barrier: identification of a uvomorulin-like polypeptide. *J. Cell Biol.* 102:457–468.
Hatae, T., M. Fujita, and K. Okuyama. 1988. Study on the origin of apical tubules in ileal absorptive cells of suckling rats using concanavalin-A as a membrane-bound tracer. *Cell Tissue Res.* 251:511–521.
Herman, B., and D. F. Albertini. 1981. A time-lapse video image intensification analysis of cytoplasmic organelles during endosomes translocation. *J. Cell Biol.* 98:565–576.
Herzog, V. 1984. Pathways of endocytosis in thyroid follicle cells. *Int. Rev. Cytol.* 91:107–139.
Hopkins, C. 1983. The importance of the endosome in intracellular traffic. *Nature (Lond.).* 305:684–685.
Langanger, G., J. De Mey, and H. Adams. 1983. 1,4-Diazobizyklo(2-2-2)'-Oktan (DABCO) verzögert das Ausbleichen von Immunofluorescensenz-präparaten. *Mikroskopie.* 40:237–241.
Lehner, C. F., V. Kurer, H. M. Eppenberger, and E. A. Nigg. 1986. The nuclear lamin protein family in higher vertebrates. *J. Biol. Chem.* 261:13293–13301.
Mostov, K. E., and N. E. Simister. 1985. Transcytosis. *Cell.* 43:389–390.
Nielsen, J. T., S. Nielsen, and E. I. Christensen. 1985. Transtubular transport of proteins in rabbit proximal tubules. *J. Ultrastruct. Res.* 92:133–145.
Oliver, C. 1982. Endocytic pathways at the lateral and basal cell surfaces of exocrine acinar cells. *J. Cell Biol.* 95:154–161.
Oliver, C., and A. R. Hand. 1978. Uptake and fate of luminally administered horseradish peroxidase in resting and isoproterenol-stimulated rat parotid acinar cells. *J. Cell Biol.* 76:207–220.
Parton, R., K. Prydz, M. Bomsel, K. Simons, and G. Griffiths. 1989. Meeting of the apical and basolateral endocytic pathways of the MDCK cells in late endosomes. Manuscript submitted for publication.
Pastan, I. H., and M. C. Willingham. 1981. Journey to the center of the cell: role of the receptosome. *Science (Wash. DC).* 214:504–509.
Richardson, J. C. W., V. Scalera, and N. L. Simmons. 1981. Identification of two strains of MDCK cells which resemble separate nephron tubule segments. *Biochim. Biophys. Acta.* 673:26–36.
Rodman, S. J., L. Seidman, and M. Gist Farquhar. 1986. The membrane composition of coated pits, microvilli, endosomes and lysosomes is distinctive in the rat kidney proximal tubule cell. *J. Cell Biol.* 102:77–87.
Sargiacomo, M., M. Lisanti, L. Graeve, A. Le Bivic, and E. Rodriguez-Boulan. 1989. Integral and peripheral protein composition of the apical and basolateral membrane domains in MDCK cells. *J. Membr. Biol.* 107:277–286.
Simons, K., and S. D. Fuller. 1985. Cell surface polarity in epithelia. *Annu. Rev. Cell Biol.* 1:243–288.
Steinman, R. M., S. E. Brodie, and Y. A. Cohn. 1976. Membrane flow during pinocytosis. A stereologic analysis. *J. Cell Biol.* 68:665–687.
Stelzer, E. H. K., R. Stricker, R. Fick, C. Storz, and P. Hänninen. 1989. Confocal fluorescence microscopes for biological research. SPIE Proc. 1028: In press.
Stevenson, B. R., J. D. Silicano, M. S. Mooseker, and D. A. Goodenough. 1986. Identification of ZO-1: a high molecular weight polypeptide associated with the tight junction (zonula occludens) in a variety of epithelia. *J. Cell Biol.* 103:755–766.
Swanson, J. A., B. D. Yirinec, and S. C. Silverstein. 1985. Phorbol esters and horseradish peroxidase stimulate pinocytosis and redirect flow of pinocytosed fluid through macrophages. *J. Cell Biol.* 100:851–859.
van Deurs, B., and E. I. Christensen. 1984. Endocytosis in kidney proximal tubules and cultured fibroblasts: a review of the structural aspect of membrane recycling between the plasma membrane and endocytic vacuoles. *Eur. J. Cell Biol.* 33:163–173.
von Bonsdorff, C.-H., S. D. Fuller, and K. Simons. 1985. Apical and basolateral endocytosis in Madin-Darby canine kidney (MDCK) cells grown on nitrocellulose filters. *EMBO (Eur. Mol. Biol. Organ.) J.* 4:2781–2792.
Wall, D. A., G. Wilson, and A. L. Hubbard. 1980. The galactose-specific recognition system of mammalian liver: the route of ligand internalization in rat hepatocytes. *Cell.* 21:79–93.